Clinical Cancer Research

A Radiomics Nomogram for the Preoperative Prediction of Lymph Node Metastasis in Bladder Cancer

Shaoxu Wu[1,2], Junjiong Zheng[1,2], Yong Li[3], Hao Yu[1,2], Siya Shi[3], Weibin Xie[1,2], Hao Liu[1,2], Yangfan Su[1,2], Jian Huang[1,2], and Tianxin Lin[1,2]

Abstract

Purpose: To develop and validate a radiomics nomogram for the preoperative prediction of lymph node (LN) metastasis in bladder cancer.

Experimental Design: A total of 118 eligible bladder cancer patients were divided into a training set ($n = 80$) and a validation set ($n = 38$). Radiomics features were extracted from arterial-phase CT images of each patient. A radiomics signature was then constructed with the least absolute shrinkage and selection operator algorithm in the training set. Combined with independent risk factors, a radiomics nomogram was built with a multivariate logistic regression model. Nomogram performance was assessed in the training set and validated in the validation set. Finally, decision curve analysis was performed with the combined training and validation set to estimate the clinical usefulness of the nomogram.

Results: The radiomics signature, consisting of nine LN status–related features, achieved favorable prediction efficacy. The radiomics nomogram, which incorporated the radiomics signature and CT-reported LN status, also showed good calibration and discrimination in the training set [AUC, 0.9262; 95% confidence interval (CI), 0.8657–0.9868] and the validation set (AUC, 0.8986; 95% CI, 0.7613–0.9901). The decision curve indicated the clinical usefulness of our nomogram. Encouragingly, the nomogram also showed favorable discriminatory ability in the CT-reported LN-negative (cN0) subgroup (AUC, 0.8810; 95% CI, 0.8021–0.9598).

Conclusions: The presented radiomics nomogram, a non-invasive preoperative prediction tool that incorporates the radiomics signature and CT-reported LN status, shows favorable predictive accuracy for LN metastasis in patients with bladder cancer. Multicenter validation is needed to acquire high-level evidence for its clinical application. *Clin Cancer Res; 23(22); 6904–11. ©2017 AACR.*

Introduction

Bladder cancer is the ninth most common cancer and the thirteenth most common cause of cancer-related death worldwide (1). Lymph node (LN) metastasis in patients with bladder cancer indicates a negative prognosis (2–4). Accurate preoperative information about LN metastasis can provide useful information for making treatment decisions, such as the extent of pelvic LN dissection (PLND) required and the use of neoadjuvant chemotherapy (5, 6). Currently, contrast-enhanced CT plays an important role in preoperative nodal staging and is a standard procedure in clinical practice (7). However, its efficacy in identifying malignant nodes is unsatisfactory, with a sensitivity of 31%–45%. This low efficacy has led to a considerable proportion of patients being understaged or overstaged (8–10).

"Radiomics" refers to the high-throughput extraction of large numbers of imaging features, thus converting medical images into mineable high-dimensional data; the subsequent quantitative analysis of these data can support decision-making (11, 12). The radiomics approach has drawn increased attention in recent years, because radiomics data may aid in disease detection, diagnosis, evaluation of prognosis, and prediction of treatment response (12). Currently, radiomics is mainly used in oncology to facilitate improved clinical decision-making, especially in lung cancer and in glioblastoma (13, 14). To our knowledge, there has been no radiomics-based study for the preoperative prediction of LN metastasis in bladder cancer to date.

Hence, in this study, we sought to develop and validate a radiomics nomogram that would incorporate a radiomics signature and clinical risk factors for the preoperative prediction of LN metastasis in patients with bladder cancer.

Materials and Methods

Patients

This retrospective analysis of anonymous data was approved by the institutional review board. A total of 118 consecutive patients with bladder cancer who were treated between July 2007 and March 2017 were enrolled in our study, according to the following inclusion criteria: (i) patients who underwent laparoscopic radical

[1]Department of Urology, Sun Yat-Sen Memorial Hospital, Sun Yat-Sen University, Guangzhou, P.R. China. [2]Guangdong Provincial Key Laboratory of Malignant Tumor Epigenetics and Gene Regulation, Sun Yat-Sen Memorial Hospital, Sun Yat-Sen University, Guangzhou, P.R. China. [3]Department of Radiology, Sun Yat-Sen Memorial Hospital, Sun Yat-Sen University, Guangzhou, P.R. China.

Note: Supplementary data for this article are available at Clinical Cancer Research Online (http://clincancerres.aacrjournals.org/).

S. Wu and J. Zheng are the co-first authors of this article.

Corresponding Authors: Tianxin Lin, Sun Yat-sen Memorial Hospital, Sun Yat-sen University, 107 W. Yanjiang Road, Guangzhou, Guangdong 510120, P.R. China. Phone: 8613-7240-08338; Fax: 8620-8133-2405; E-mail: tianxinl@sina.com; and J. Huang, urolhj@sina.com

doi: 10.1158/1078-0432.CCR-17-1510

Translational Relevance

Radiomics, a promising field, uses computational methods to convert medical images into mineable high-dimensional data, which may aid in disease detection, diagnosis, evaluation of prognosis, and prediction of treatment response. In this study, a radiomics nomogram for the preoperative prediction of lymph node (LN) metastasis in bladder cancer that incorporated the radiomics signature and CT-reported LN status was developed, which showed good calibration and discrimination in the training and validation set. The nomogram also showed favorable discriminatory ability with the CT-reported LN-negative (cN0) subgroup. This radiomics-based study (i) provides a noninvasive and low cost preoperative prediction tool to identify the bladder cancer patients with high risk of LN metastasis; and (ii) provides novel insights into the construction of a predictive model for bladder cancer patients.

cystectomy and extended PLND (up to the aortic bifurcation) for bladder cancer with tumor tissues that were pathologically confirmed as urothelial carcinoma; (ii) contrast-enhanced pelvic CT performed fewer than 20 days before surgery; and (iii) availability of clinical characteristics. The exclusion criteria were as follows: (i) preoperative therapy (neoadjuvant chemotherapy or radiotherapy), and (ii) suffering from other tumor disease at the same time. Supplementary Figure S1 shows the patient recruitment pathway. We divided the patients into two independent sets: 80 patients treated between July 2007 and June 2014 constituted the training set, whereas 38 patients treated between July 2014 and March 2017 constituted the validation set.

Clinical data, such as age and sex, were obtained by reviewing the medical records. All CT scans were reviewed by two radiologists with, respectively 15 (Y. Li, reader 1) and 10 years (Zhuo Wu, Department of Radiology, Sun Yat-Sen Memorial Hospital, Sun Yat-Sen University, Guangzhou, P.R. China, reader 2) of experience in pelvic CT interpretation. They recorded the size of the largest tumor, the number of tumors, T staging, and the size of all visible LNs. Patients with visible pelvic LN > 8 mm or abdominal LN > 10 mm in the maximal short-axis diameter were regarded as clinically LN-positive (cN+; ref. 15). Any disagreement was resolved by consultation. The 2009 TNM staging system (16) and the 2004 WHO classification (17) were used for pathologic staging and pathologic grading, respectively.

CT image acquisition, region-of-interest segmentation, and radiomic feature extraction

The radiomics workflow is presented in Fig. 1. Before receiving transurethral resection of bladder tumor (TURBT), all patients underwent contrast-enhanced pelvic CT with a 64-slice spiral CT scanner (Somatom Sensation 64, Siemens Medical Systems). The CT scan parameters were as follows: 120 kV, 200 effective mAs, beam collimation of 64 × 0.6 mm, a matrix of 512 × 512, a pitch of 0.8, and a gantry rotation time of 0.5 s. After nonenhanced CT scanning, a dynamic contrast-enhanced CT scan was performed

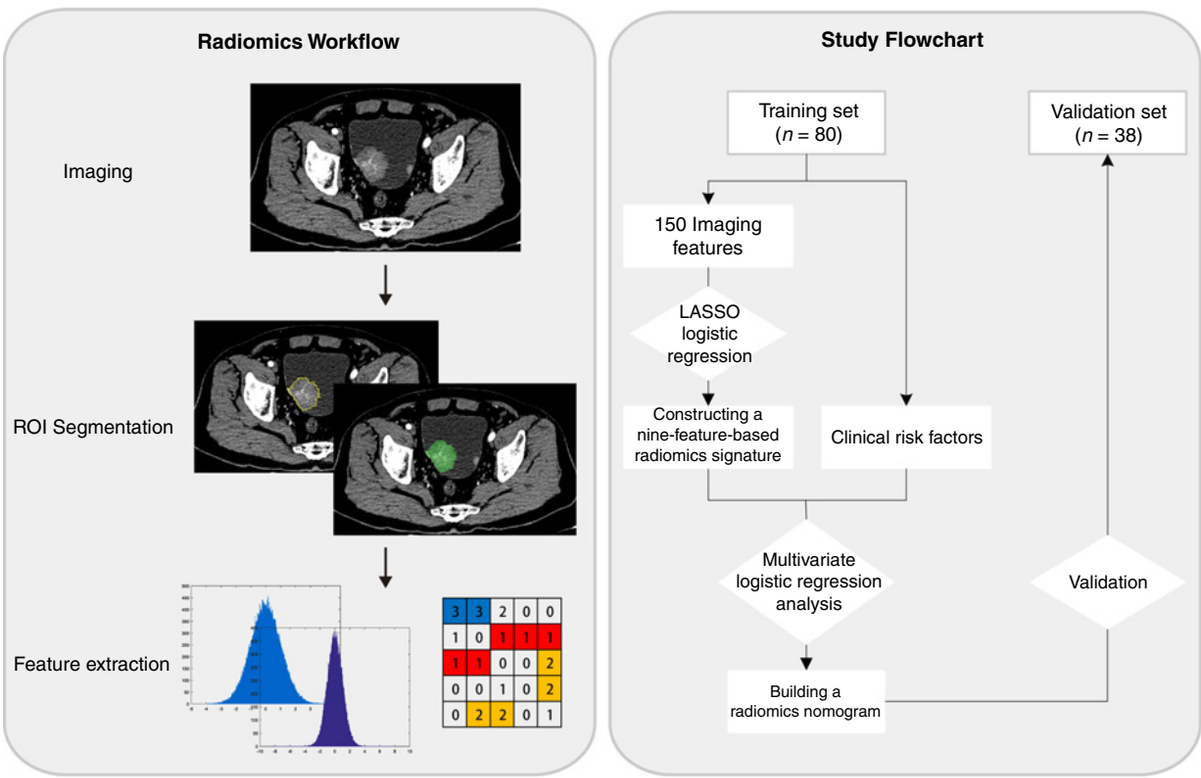

Figure 1.
Radiomics workflow and study flowchart.

after intravenous administration of 80–100 mL nonionic contrast material (Iopamidol, 370 mg I/mL, Bracco) using power injection at a rate of 3.5 mL/second followed by saline flush (20 mL). Arterial-phase and vein-phase images were obtained at 25 and 60 seconds, respectively. The slice thickness of the reconstructed image was 1.0 mm. Arterial-phase CT images were retrieved for image feature extraction.

Tumor regions of interest (ROI) were semiautomatically segmented in the largest cross-sectional area using the Materialise MIMICS 17.0 software (Materialise). Texture extraction was performed using in-house texture extraction software with algorithms implemented in MATLAB 2015b (MathWorks). In total, 150 imaging features were extracted from a single CT image, including 50 gray-level histogram features and 100 gray-level cooccurrence matrix features. More information about the ROI segmentation procedure and radiomics feature extraction methodology can be found in the Supplementary Data.

Intra- and interclass correlation coefficients (ICC) were used to assess the intra- and interobserver reproducibility of radiomics feature extraction. We initially chose 25 random CT images for ROI segmentation and feature extraction. The ROI segmentation was performed by two radiologists with, respectively, 15 (reader 1) and 10 years (reader 2) of experience in pelvic CT interpretation. Reader 1 then repeated the same procedure one week later. An ICC greater than 0.75 indicates good agreement of the feature extraction. The remaining image segmentation was performed by reader 1.

LN status–related feature selection and radiomics signature construction

We used the least absolute shrinkage and selection operator (LASSO) logistic regression algorithm, which is suitable for the regression of high-dimensional data, with the training set to select LN status–related features with nonzero coefficients from among the 150 imaging features (18). A formula was generated using a linear combination of selected features that were weighted by their respective LASSO coefficients; the formula was then used to calculate a risk score (defined as the radiomics score) for each patient to reflect the risk of LN metastasis. The predictive accuracy of the radiomics signature was quantified by the area under the receiver–operator characteristic (ROC) curve (AUC) in both the training and validation sets.

Construction of the radiomics nomogram

The radiomics signature and the clinical variables were tested in a multivariate logistic regression model to predict LN metastasis in the training set. Regarding the multivariate logistic regression, the collinearity diagnosis was performed using the variance inflation factor (VIF). A radiomics nomogram was then constructed on the basis of the multivariate logistic regression model.

Assessment of nomogram performance

The calibration of the nomogram was assessed with a calibration curve. The Hosmer–Lemeshow test was performed to assess the goodness-of-fit of the nomogram, and the AUC was calculated to quantify the discrimination performance of the nomogram.

Internal validation of the radiomics nomogram

Internal validation of the radiomics nomogram was performed with the validation set. A radiomics score was calculated for each patient in the validation set using the formula constructed in the training set. The calibration and the Hosmer–Lemeshow test were performed, and the AUC was calculated.

Clinical utility of the radiomics nomogram

To estimate the clinical utility of the nomogram, decision curve analysis (DCA) was performed by calculating the net benefits for a range of threshold probabilities in the combined training and validation set.

Statistical analysis

The LASSO logistic regression model was used with penalty parameter tuning that was conducted by 10-fold cross-validation based on minimum criteria. The likelihood ratio test with backward step-down selection was applied to the multivariate logistic regression model. Detailed descriptions of the LASSO algorithm and DCA are provided in the Supplementary Data.

All statistical tests were performed using R statistical software version 3.3.1. We used the "glmnet" package to perform the LASSO logistic regression model analysis. The VIFs were calculated using the "car" package. The ROC curves were plotted using the "pROC" package. Nomogram construction and calibration plots were performed using the "rms" package, and the Hosmer–Lemeshow test was conducted using the "generalhoslem" package. DCA was performed using the "dca.R." A two-sided $P < 0.05$ was considered significant.

Results

The study flowchart is presented in Fig. 1. The patient characteristics in the training and validation sets are shown in Table 1 and Supplementary Table S1. pN1–3 patients formed 21.3% (17/80) and 18.4% (7/38) of the training and validation sets, respectively, and there were no significant differences between them ($P = 0.721$, χ^2 test). In total, 58.3% (14/24) of the pN1–3 patients were understaged and 7.4% (7/94) of the pN0 patients were overstaged according to the CT-reported LN status in our study.

Table 1. Baseline characteristics of the training and validation sets

	Training set ($n = 80$)			Validation set ($n = 38$)		
	pN1-3	pN0	P^a	pN1-3	pN0	P^a
Gender						
Male	16	44	0.083	6	24	1.000
Female	1	19		1	7	
Age, years						
<65	10	37	0.994	2	17	0.405
≥65	7	26		5	14	
CT-reported tumor size						
≤3 cm	7	33	0.412	2	15	0.427
>3 cm	10	30		5	16	
CT-reported number of tumors						
Single	13	38	0.219	4	16	1.000
Multiple	4	25		3	15	
CT-reported T stage						
cTa-cT2	4	34	0.026[b]	0	21	0.002[b]
cT3-cT4	13	29		7	10	
CT-reported LN status						
cN1-3	5	4	0.025[b]	5	3	0.002[b]
cN0	12	59		2	28	

[a]*P* values were obtained from the univariate association analyses between the LN status and each clinical factor.
[b]$P < 0.05$.

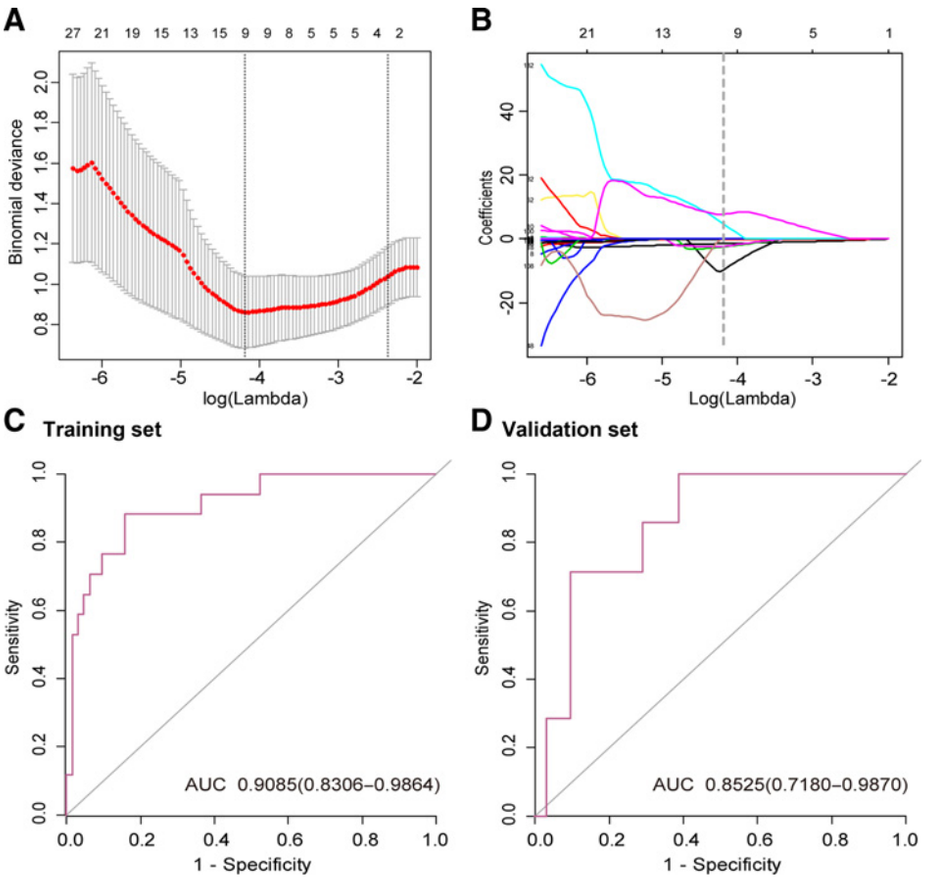

Figure 2.
Texture feature selection using LASSO logistic regression and the predictive accuracy of the radiomics signature. **A,** Selection of the tuning parameter (λ) in the LASSO model via 10-fold cross-validation based on minimum criteria. Binomial deviances from the LASSO regression cross-validation procedure were plotted as a function of log(λ). The *y*-axis indicates binomial deviances. The lower *x*-axis indicates the log(λ). Numbers along the upper *x*-axis represent the average number of predictors. Red dots indicate average deviance values for each model with a given λ, and vertical bars through the red dots show the upper and lower values of the deviances. The vertical black lines define the optimal values of λ, where the model provides its best fit to the data. The optimal λ value of 0.015 with log(λ) = −4.18 was selected. **B,** LASSO coefficient profiles of the 150 texture features. The dotted vertical line was plotted at the value selected using 10-fold cross-validation in **A**. The nine resulting features with nonzero coefficients are indicated in the plot. Plots (**C**) and (**D**) show the ROC curves of the radiomics signature in the training and validation sets, respectively.

A total of 150 imaging features were extracted from each arterial-phase CT image. The features were classified into two categories: gray-level histogram features and gray-level cooccurrence matrix features. More-detailed information about the imaging features can be found in the Supplementary Methods and Supplementary Table S2. The intraobserver ICCs ranged from 0.803 to 0.990 and the interobserver ICCs ranged from 0.779 to 0.935, indicating favorable intra- and interobserver feature extraction reproducibility.

Nine LN status–related features with nonzero coefficients were screened using a LASSO logistic regression model in the training set (Fig. 2A and B). The radiomics score calculation formula is presented in the Supplementary Data, where the selected features can be found. pN1–3 patients generally displayed a higher radiomics score than pN0 patients. There was a significant difference between the radiomics scores [median (interquartile range)] of the pN0 and pN1-3 patient groups in the training set [−2.271 (−3.484 to −1.439) vs. 0.113 (−0.722–0.486), respectively, $P < 0.001$]; this difference was confirmed in the validation set [−2.505 (−3.056 to −0.811) vs. −0.386 (−0.963–1.247), respectively, $P < 0.05$]. The radiomics signature showed favorable predictive efficacy, with an AUC of 0.9085 [95% confidence interval (CI), 0.8306–0.9864] in the training set and 0.8525 (95% CI, 0.7180–0.9870) in the validation set (Fig. 2C and D).

The radiomics signature and CT-reported LN status were identified as independent predictors of LN metastasis in bladder cancer patients by a multivariate logistic regression model (Table 2). Regarding the collinearity diagnosis, the VIFs of the seven predictors ranged from 1.09 to 1.28, indicating that there was no collinearity. A radiomics nomogram incorporating these

Table 2. Risk factors for LN metastasis in bladder cancer

	Univariate logistic regression		Multivariate logistic regression	
Variable and intercept	**OR (95% CI)**	***P***	**OR (95% CI)**	***P***
The radiomics score (per 0.1 increase)	1.167 (1.081–1.260)	<0.001[a]	1.171 (1.080–1.269)	<0.001[a]
Gender (male vs. female)	0.145 (0.018–1.171)	0.070	NA	NA
Age, years (<65 vs. ≥65)	0.996 (0.335–2.958)	0.994	NA	NA
CT-reported tumor size (≤3 cm vs. >3 cm)	1.571 (0.531–4.651)	0.414	NA	NA
CT-reported number of tumors (single vs. multiple)	0.468 (0.137–1.599)	0.226	NA	NA
CT-reported T stage (cTa-cT2 vs. cT3-cT4)	3.810 (1.119–12.975)	0.032[a]	NA	NA
CT-reported LN status (cN0 vs. cN1-3)	6.146 (1.436–26.303)	0.014[a]	10.515 (1.069–103.459)	0.044[a]

NOTE: NA, not available. These variables were eliminated in the multivariate logistic regression model, so the OR and *P* values were not available.
[a]$P < 0.05$.

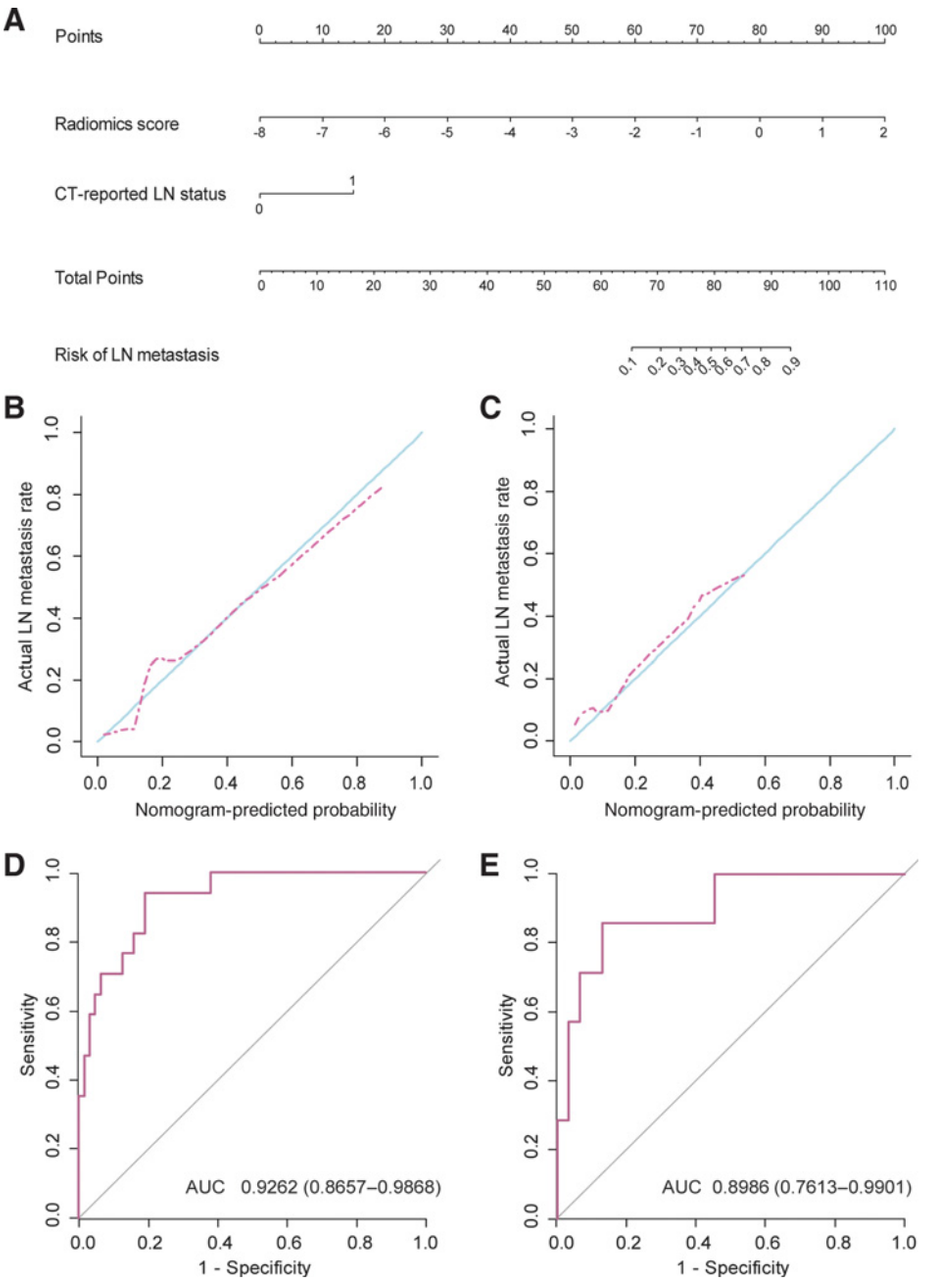

Figure 3.
Radiomics nomogram for the prediction of LN metastasis (**A**). Calibration curves of the radiomics nomogram in the training set (**B**) and validation set (**C**). Calibration curves depict the calibration of the nomogram in terms of agreement between the predicted risk of LN metastasis and observed pN outcomes. The 45° blue line represents a perfect prediction, and the dotted lines represent the predictive performance of the nomogram. The closer the dotted line fit is to the ideal line, the better the predictive accuracy of the nomogram is. Plots (**D**) and (**E**) show the ROC curves of the radiomics nomogram in the training and validation sets, respectively.

two predictors was constructed (Fig. 3A). Figure 3B illustrates the calibration curve of the nomogram. The calibration curve and a nonsignificant Hosmer–Lemeshow test statistic ($P = 0.6521$) showed good calibration in the training set. An AUC of 0.9262 (95% CI, 0.8657–0.9868) also revealed good discrimination by the nomogram (Fig. 3D). The favorable calibration of the radiomics nomogram was confirmed with the validation set (Fig. 3C). The Hosmer–Lemeshow test yielded a nonsignificant P value of 0.5359, and the AUC of the validation set was 0.8986 (95% CI, 0.7613–0.9901; Fig. 3E). Therefore, our nomogram performed well in both the training and validation sets.

The DCA for the radiomics nomogram is presented in Fig. 4. The DCA indicated that when the threshold probability for a doctor or a patient is within a range from 0 to 0.84, the radiomics nomogram adds more net benefit than the "treat all" or "treat none" strategies.

In addition, we evaluated the discriminatory efficiency of the radiomics nomogram in all 118 patients and in the CT-reported LN-negative (cN0) subgroup ($n = 101$) using ROC analyses. Figure 5A shows ROC analyses comparing the discriminatory efficacy of the radiomics nomogram to those of the radiomics signature and the CT-reported LN status alone. The radiomics nomogram yielded the greatest ROC of 0.9109 (95% CI, 0.8538–0.9680), which suggested that the nomogram achieved better predictive efficacy than either the radiomics signature or the CT-reported LN status alone. Notably, the nomogram also

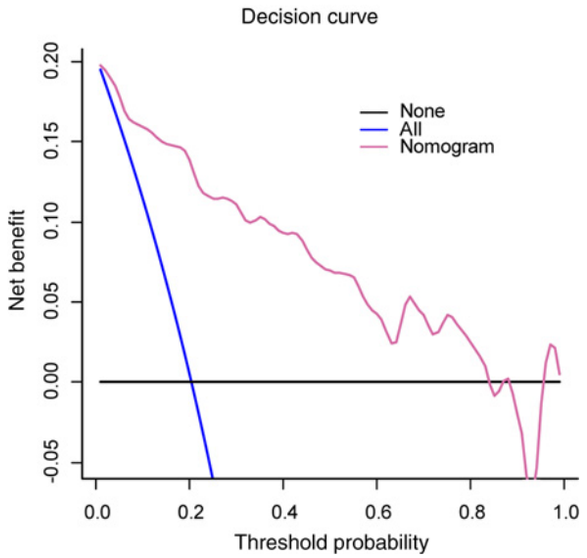

Figure 4.

DCA for the radiomics nomogram. The *y*-axis represents the net benefit. The pink line represents the radiomics nomogram. The blue line represents the hypothesis that all patients had LN metastases. The black line represents the hypothesis that no patients had LN metastases. The *x*-axis represents the threshold probability. The threshold probability is where the expected benefit of treatment is equal to the expected benefit of avoiding treatment. For example, if the possibility of LN metastasis involvement of a patient is over the threshold probability, then a treatment strategy for LN metastasis should be adopted. The decision curves in the validation set showed that if the threshold probability is between 0 and 0.84, then using the radiomics nomogram to predict LN metastases adds more benefit than treating either all or no patients.

showed good discriminatory ability in the cN0 subgroup (AUC 0.8810; 95% CI, 0.8021–0.9598; Fig. 5C). After obtaining the risk scores from the nomogram, we defined an optimal risk score cutoff value of −1.412, based on the maximum Youden index in the training set. The patients were classified into low- and high-risk groups according to the optimal cut-off values. Notably, the high-risk group had a greater possibility of LN metastasis in all patients and in the cN0 subgroup (Fig. 5B and D).

Discussion

LN metastasis is a negative prognostic factor in patients with bladder cancer. Patients with LN metastasis have a lower 5-year overall survival rate (15–31%) than LN-negative patients (>60%; refs. 2–4). Preoperative prediction of LN status in patients with bladder cancer is therefore important for clinical decision-making.

A phase III randomized trial revealed that patients with muscle-invasive bladder cancer (MIBC) show improved 10-year survival after neoadjuvant chemotherapy (36% vs. 30% without; ref. 19). In addition, current guidelines recommend offering neoadjuvant chemotherapy to T2–T4a and cN0M0 bladder cancer patients (20). However, a large proportion of bladder cancer patients will not benefit from neoadjuvant chemotherapy, and it is currently difficult to identify the patients who will benefit (21). Therefore, neoadjuvant chemotherapy has not been performed regularly (22). Moreover, because neoadjuvant chemotherapy targets micrometastasis (including LN metastasis), patients with LN metastases are likely to benefit from this therapy (23).

Knowledge has grown regarding bilateral PLND at the time of radical cystectomy in patients with bladder cancer. However, controversy remains concerning the extent to which PLND should be performed. A larger PLND template can provide more accurate nodal staging and lead to more radical therapy. Dorin and colleagues reported on a series of 646 patients who received radical cystectomy and PLND. They found that 23% of the patients showed LN metastasis, among whom 41% had malignant LNs above the bifurcation of the common iliac arteries, exceeding the region of the standard PLND template (24). A systematic review indicated that extended PLND might be superior to lesser degrees of dissection (25). Nevertheless, extended PLND has not been performed regularly or widely because more extended PLND has a higher grade of operative difficulty and, hence, the potential for more harm. Currently, clinicians cannot identify patients who will benefit from extended PLND.

If patients who are at high risk of LN metastasis can be identified preoperatively, then such patients might represent an appropriate group for neoadjuvant chemotherapy and extended PLND. However, the accuracy of contrast-enhanced CT, which is the standard clinical procedure for preoperative nodal staging, is unsatisfactory, and a considerable proportion of patients are understaged or overstaged (7–10). Thus, improved predictive tools for preoperative nodal staging are urgently needed.

A nomogram incorporating two items, namely "TUR T stage" and "TUR tumor grade," has been reported to preoperatively predict LN stage. The predictive accuracy of this model is only 63.1%, thus suggesting that 36.7% of patients would remain misclassified (26). With the development of high-throughput technology and analytical approaches, multimarker analysis has been increasingly applied. This approach combines individual markers to generate marker panels for better predictive or diagnostic performance and has been a subject of much interest in recent years (27). For example, a 20 mRNA-based classifier [AUC (95% CI), 0.67 (0.60–0.75)] and a 51 RNA–based classifier [AUC (95% CI), 0.82 (0.71–0.93)] have been constructed to predict LN metastasis in bladder cancer patients (28, 29). Similarly, the radiomics approach can incorporate individual imaging features into a radiomics signature. Zhang and colleagues proposed a radiomics strategy based on the texture features of diffusion-weighted images for preoperative grading in patients with bladder cancer (30). That study, which represents the first radiomics-based study of bladder cancer demonstrated the feasibility of applying a radiomics approach to bladder cancer.

Thus, we attempted to develop a radiomics signature for the prediction of LN metastasis in patients with bladder cancer. Our radiomics signature exhibited favorable discrimination, with an AUC of 0.8901 across all 118 patients. Next, we considered clinical risk factors. A multivariate logistic regression model indicated that CT-reported LN status was a significant predictive factor distinct from the radiomics signature. To provide an easy-to-use tool for clinicians, we constructed a radiomics nomogram based on a multivariate logistic regression model that showed good calibration and discrimination in the training and validation sets. The AUC of the nomogram was 0.9109, suggesting that the radiomics nomogram achieved greater predictive efficacy than either the radiomics signature or the CT-reported LN status alone. Notably, a valuable feature of our radiomics nomogram is its discriminatory ability in cN0 patients. Bladder cancer patients

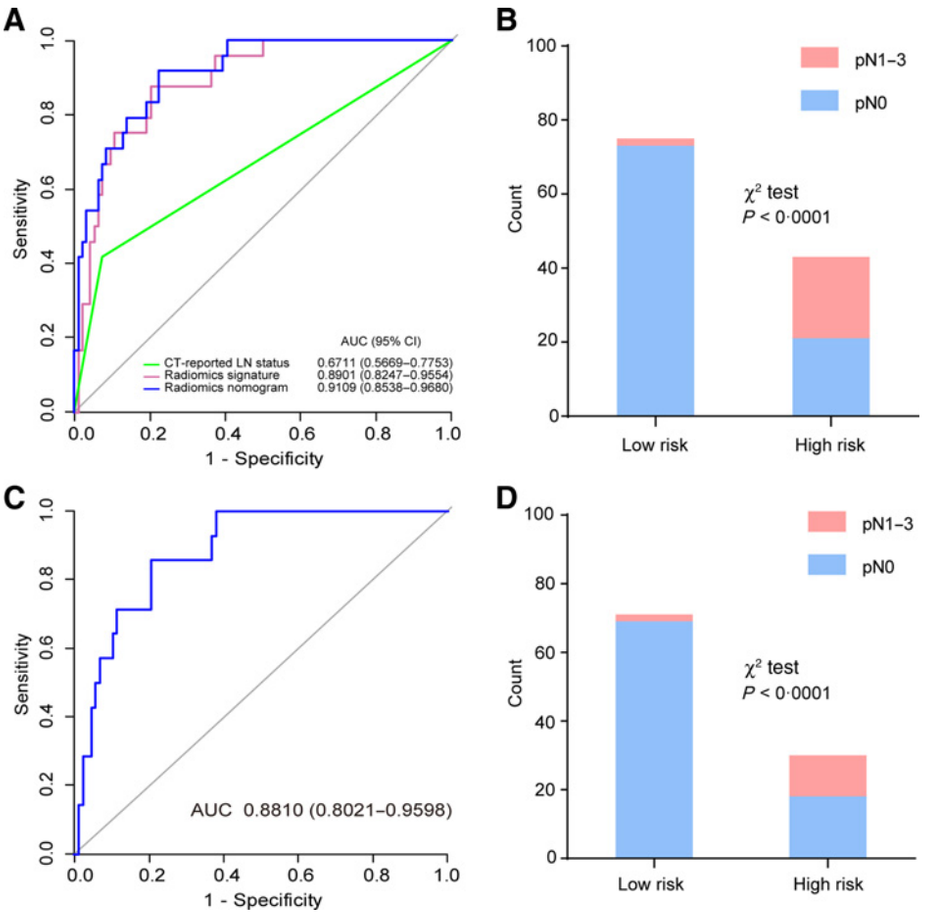

Figure 5.
Performance of the nomogram in all 118 patients and in the cN0 subgroup ($n = 101$). The left panels present the ROC curve analyses for the nomogram. The right panels show the risk-classification performance of the nomogram. **A** and **B,** All 118 patients. **C** and **D,** cN0 subgroup.

diagnosed as cN0 are typically considered to be at low risk of LN metastasis. However, some cN0 patients actually harbor LN metastases, and it is a formidable challenge to precisely identify which patients will experience LN metastasis. Encouragingly, our nomogram showed good discriminatory ability in cN0 patients. Furthermore, when categorized into low- and high-risk groups on the basis of the cutoff values of the risk score derived from the nomogram, the high-risk group had a significantly greater probability of having LN metastases. Therefore, our nomogram may serve as an accurate and reliable predictive tool for LN metastasis in patients with bladder cancer, especially cN0 patients.

Compared with contrast-enhanced CT, which is the standard clinical nodal staging tool in current clinical practice, the predictive power of our model is clearly superior. For cN0 patients in particular, our nomogram exhibits superior performance. On the basis of contrast-enhanced CT, cN0 patients are all diagnosed as LN-negative, whereas our nomogram showed good discriminatory ability to identify the patients at high risk of LN metastasis. Notably, the three previous models for preoperative nodal staging were invasive predictive tools. The presented radiomics nomogram consists of only two items, both of which are available from routine contrast-enhanced CT. Thus, our nomogram can serve as a noninvasive preoperative predictive tool to assess LN status in bladder cancer patients. In addition, the predictive power of our model for nodal staging is superior to the three previous models.

The limitations of our study include the lack external validation for the model. Multicenter validation with a larger sample size is needed to acquire high-level evidence for clinical application. In addition, genetic markers have not yet been incorporated into our nomogram. Because multigene classifiers have reportedly performed well in bladder cancer preoperative nodal staging (28, 29), a combination of gene marker panels and a radiomics signature may improve the ability to predict LN metastasis in patients with bladder cancer.

Our radiomics nomogram, which is a noninvasive predictive tool that combines a radiomics signature with CT-reported LN status, shows favorable predictive accuracy for preoperative LN metastasis in bladder cancer, especially for cN0 patients. Multicenter retrospective validation, even prospective randomized clinical trials should be performed to obtain high-level evidence for clinical applications in subsequent studies.

Disclosure of Potential Conflicts of Interest

No potential conflicts of interest were disclosed.

Authors' Contributions

Conception and design: S. Wu, J. Zheng, J. Huang, T. Lin
Development of methodology: S. Wu, J. Zheng, Y. Li
Acquisition of data (provided animals, acquired and managed patients, provided facilities, etc.): H. Yu, S. Shi, W. Xie, H. Liu, Y. Su
Analysis and interpretation of data (e.g., statistical analysis, biostatistics, computational analysis): S. Wu, J. Zheng, Y. Li
Writing, review, and/or revision of the manuscript: S. Wu, J. Zheng, J. Huang, T. Lin

Administrative, technical, or material support (i.e., reporting or organizing data, constructing databases): H. Yu, S. Shi, W. Xie, H. Liu, Y. Su
Study supervision: J. Huang, T. Lin

Grant Support

This work was funded by the National Natural Science Foundation of China (81572514, U1301221, 81472384, 81402106, 81372729, 81272808, and 81172431), the National Natural Science Foundation of Guangdong (2016A030313321, 2015A030311011, 2015A030310122, S2013020012671, 07117336, and 10151008901000024), the Grant [2013]163 from Key Laboratory of Malignant Tumor Molecular Mechanism and Translational Medicine of Guangzhou Bureau of Science and Information Technology, the Grant KLB09001 from the Key Laboratory of Malignant Tumor Gene Regulation and Target Therapy of Guangdong Higher Education Institutes, and the Grant from Guangdong Science and Technology Department (2015B050501004).

The costs of publication of this article were defrayed in part by the payment of page charges. This article must therefore be hereby marked *advertisement* in accordance with 18 U.S.C. Section 1734 solely to indicate this fact.

Received May 26, 2017; revised July 15, 2017; accepted August 30, 2017; published OnlineFirst September 5, 2017.

References

1. Antoni S, Ferlay J, Soerjomataram I, Znaor A, Jemal A, Bray F. Bladder cancer incidence and mortality: a global overview and recent trends. Eur Urol 2017;71:96–108.
2. Bassi P, Ferrante GD, Piazza N, Spinadin R, Carando R, Pappagallo G, et al. Prognostic factors of outcome after radical cystectomy for bladder cancer: a retrospective study of a homogeneous patient cohort. J Urol 1999;161: 1494–7.
3. Karl A, Carroll PR, Gschwend JE, Knuchel R, Montorsi F, Stief CG, et al. The impact of lymphadenectomy and lymph node metastasis on the outcomes of radical cystectomy for bladder cancer. Eur Urol 2009;55:826–35.
4. Zehnder P, Studer UE, Daneshmand S, Birkhauser FD, Skinner EC, Roth B, et al. Outcomes of radical cystectomy with extended lymphadenectomy alone in patients with lymph node-positive bladder cancer who are unfit for or who decline adjuvant chemotherapy. BJU Int 2014;113:554–60.
5. Kluth LA, Black PC, Bochner BH, Catto J, Lerner SP, Stenzl A, et al. Prognostic and prediction tools in bladder cancer: a comprehensive review of the literature. Eur Urol 2015;68:238–53.
6. Zargar-Shoshtari K, Zargar H, Lotan Y, Shah JB, van Rhijn BW, Daneshmand S, et al. A multi-institutional analysis of outcomes of patients with clinically node positive urothelial bladder cancer treated with induction chemotherapy and radical cystectomy. J Urol 2016;195:53–9.
7. McKibben MJ, Woods ME. Preoperative imaging for staging bladder cancer. Curr Urol Rep 2015;16:22.
8. Goodfellow H, Viney Z, Hughes P, Rankin S, Rottenberg G, Hughes S, et al. Role of fluorodeoxyglucose positron emission tomography (FDG PET)-computed tomography (CT) in the staging of bladder cancer. BJU Int 2014;114:389–95.
9. Lodde M, Lacombe L, Friede J, Morin F, Saourine A, Fradet Y. Evaluation of fluorodeoxyglucose positron-emission tomography with computed tomography for staging of urothelial carcinoma. BJU Int 2010;106:658–63.
10. Baltaci S, Resorlu B, Yagci C, Turkolmez K, Gogus C, Beduk Y. Computerized tomography for detecting perivesical infiltration and lymph node metastasis in invasive bladder carcinoma. Urol Int 2008;81:399–402.
11. Lambin P, Rios-Velazquez E, Leijenaar R, Carvalho S, van Stiphout RG, Granton P, et al. Radiomics: extracting more information from medical images using advanced feature analysis. Eur J Cancer 2012;48:441–6.
12. Gillies RJ, Kinahan PE, Hricak H. Radiomics: images are more than pictures, they are data. Radiology 2016;278:563–77.
13. Lee G, Lee HY, Park H, Schiebler ML, van Beek EJ, Ohno Y, et al. Radiomics and its emerging role in lung cancer research, imaging biomarkers and clinical management: State of the art. Eur J Radiol 2017;86:297–307.
14. Kotrotsou A, Zinn PO, Colen RR. Radiomics in brain tumors: an emerging technique for characterization of tumor environment. Magn Reson Imaging Clin N Am 2016;24:719–29.
15. Dorfman RE, Alpern MB, Gross BH, Sandler MA. Upper abdominal lymph nodes: criteria for normal size determined with CT. Radiology 1991;180: 319–22.
16. Sobin LH, Gospodarowicz M, Wittekind C. TNM classification of malignant tumors. Hoboken, NJ: Wiley Blackwell; 2009.
17. Epstein J, Eble J, Sauter G, Sesterhenn I. World Health Organization Classification of tumors: pathology and genetics of tumours of the urinary system and male genital organs; 2004.
18. Tibshirani R. Regression shrinkage and selection via the lasso. J R Stat Soc Ser B (Methodol) 1996;58:267–88.
19. Griffiths G, Hall R, Sylvester R, Raghavan D, Parmar MK. International phase III trial assessing neoadjuvant cisplatin, methotrexate, and vinblastine chemotherapy for muscle-invasive bladder cancer: long-term results of the BA06 30894 trial. J Clin Oncol 2011;29:2171–7.
20. Alfred Witjes J, Lebret T, Comperat EM, Cowan NC, De Santis M, Bruins HM, et al. Updated 2016 EAU guidelines on muscle-invasive and metastatic bladder cancer. Eur Urol 2017;71:462–75.
21. Neoadjuvant chemotherapy for invasive bladder cancer. Cochrane Database Syst Rev2005:Cd005246.
22. Martini T, Gilfrich C, Mayr R, Burger M, Pycha A, Aziz A, et al. The use of neoadjuvant chemotherapy in patients with urothelial carcinoma of the bladder: current practice among clinicians. Clin Genitourin Cancer 2017;15:356–62.
23. Mertens LS, Meijer RP, Meinhardt W, van der Poel HG, Bex A, Kerst JM, et al. Occult lymph node metastases in patients with carcinoma invading bladder muscle: incidence after neoadjuvant chemotherapy and cystectomy vs after cystectomy alone. BJU Int 2014;114:67–74.
24. Dorin RP, Daneshmand S, Eisenberg MS, Chandrasoma S, Cai J, Miranda G, et al. Lymph node dissection technique is more important than lymph node count in identifying nodal metastases in radical cystectomy patients: a comparative mapping study. Eur Urol 2011;60:946–52.
25. Bruins HM, Veskimae E, Hernandez V, Imamura M, Neuberger MM, Dahm P, et al. The impact of the extent of lymphadenectomy on oncologic outcomes in patients undergoing radical cystectomy for bladder cancer: a systematic review. Eur Urol 2014;66:1065–77.
26. Karakiewicz PI, Shariat SF, Palapattu GS, Perrotte P, Lotan Y, Rogers CG, et al. Precystectomy nomogram for prediction of advanced bladder cancer stage. Eur Urol 2006;50:1254–60.
27. Birkhahn M, Mitra AP, Cote RJ. Molecular markers for bladder cancer: the road to a multimarker approach. Expert Rev Anticancer Ther 2007;7: 1717–27.
28. Smith SC, Baras AS, Dancik G, Ru Y, Ding KF, Moskaluk CA, et al. A 20-gene model for molecular nodal staging of bladder cancer: development and prospective assessment. Lancet Oncol 2011;12:137–43.
29. Seiler R, Lam LL, Erho N, Takhar M, Mitra AP, Buerki C, et al. Prediction of lymph node metastasis in patients with bladder cancer using whole transcriptome gene expression signatures. J Urol 2016;196:1036–41.
30. Zhang X, Xu X, Tian Q, Li B, Wu Y, Yang Z, et al. Radiomics assessment of bladder cancer grade using texture features from diffusion-weighted imaging. J Magn Reson Imaging 2017 [Epub ahead of print].